

# Quantifying Unmixedness in Lean Premixed Combustors Operating at High-Pressure, Fired Conditions

J. C. Barnes\* and A. M. Mellor†  
Vanderbilt University, Nashville, Tennessee 37235

Lean premixed combustor manufacturers require premixer concepts that provide homogeneity (mixedness) of the fuel that burns in the main flame. Ideally, premixer evaluation would be conducted under realistic combustor operating conditions. However, current techniques typically are limited to cold-flow, moderate-pressure (<15 atm) conditions or comparison of measured NO<sub>x</sub> emissions with others obtained in premixed systems. Thus, a simple, consistent method for quantifying unmixedness in lean premixed combustors operating at high-pressure, fired operating conditions is proposed here, using the characteristic time model developed in a previous paper.

## Nomenclature

C	= carbon
$\bar{C}$	= time mean fuel mole fraction measured at a point in the premixer exit plane
$C_{av}$	= fuel mole fraction computed assuming perfect premixing of the main fuel and air flows
CH <sub>4</sub>	= methane
CO	= carbon monoxide
COEI	= carbon monoxide emissions index, g CO/kg fuel
COEI <sub>eq</sub>	= computed equilibrium COEI, g CO/kg fuel
COEI <sub>eq,s</sub>	= computed equilibrium COEI at unmixedness of $s$ , g CO/kg fuel
H	= hydrogen atom
H/C	= hydrogen to carbon ratio
$m$	= slope of a linear equation
NO	= nitric oxide
NO <sub>x</sub>	= oxides of nitrogen, NO and NO <sub>2</sub>
NO <sub>x</sub> EI	= oxides of nitrogen emissions index, g NO <sub>2</sub> /kg fuel
NO <sub>2</sub>	= nitrogen dioxide
OH	= hydroxyl radical
$p$	= pressure, atm
$R$	= universal gas constant, cal/gmol K
$r$	= correlation coefficient
$s$	= standard deviation in equivalence ratio about $\bar{\phi}_m$ divided by $\bar{\phi}_m$
$T$	= temperature, K
$T_{\phi,m}$	= adiabatic flame temperature at the main equivalence ratio ( $\bar{\phi}_m$ ), K
$\rho$	= density, kg/m <sup>3</sup>
$\sigma_y$	= standard deviation of the $y$ values for the observed $x$ values
$\sigma_\phi$	= standard deviation in equivalence ratio about $\bar{\phi}_m$
$\tau_{res}$	= combustor residence time based on reference velocity, ms
$\tau_{sl,tno}$	= characteristic fluid time for total NO formation, ms
$\tau_{tno}$	= characteristic kinetic time for total NO formation, ms

$\phi$	= overall combustor equivalence ratio based on total air and fuel flow rates
$\phi^*$	= equivalence ratio above which CO emissions are in equilibrium
$\phi_{eddy}$	= local equivalence ratio of a single eddy
$\bar{\phi}_m$	= equivalence ratio computed assuming perfect premixing of the main fuel and airflow
$\Psi(\phi_{eddy})$	= probability density function corresponding to a time-averaged spatial distribution in equivalence ratio in a lean premixed flame

## Subscripts

$a$	= air
eddy	= single reacting eddy
$f$	= fuel
in	= inlet value
$m$	= flow through the main injector (i.e., the premixer)
$\phi < 1$	= lean premixed flame

## Introduction

LEAN premixed (LP) combustion is a technique for pollutant emissions control that is seeing increased application in gas turbines as an alternative to conventional, diffusion flame combustion. In the low-emissions mode, an ideal combustor of this type produces a homogeneous, lean fuel/air mixture and thereby eliminates the stoichiometric eddies found in conventional, diffusion-flame combustors. However, it is usually the case in LP combustors that the fuel and air are not perfectly premixed. Therefore, emissions from LP combustors<sup>1–4</sup> are not as low as experiments such as the well-controlled, “perfectly premixed” flameholder experiments<sup>5</sup> indicate that they could be.

To perform testing of candidate premixer designs, an accurate, reliable method of quantifying fuel/air mixedness in the premixer is required. Here, following a review of current techniques for evaluating fuel/air mixing in LP combustors, a technique for deducing unmixedness from combustor emissions measurements is proposed.

## Current Techniques for Evaluating Mixedness

### Computational Fluid Dynamics

Computational fluid dynamics (CFD) codes have been used to predict the extent of fuel/air mixing in a premixer module. Typically, the three-dimensional Reynolds-averaged forms of the mass, momentum, energy, and species conservation equations are solved along with the two-equation  $k$ - $\epsilon$  model,<sup>6</sup> assuming nonreacting flow. Initial conditions required in a gas-

Received Sept. 2, 1997; revision received April 15, 1998; accepted for publication April 23, 1998. Copyright © 1998 by J. C. Barnes and A. M. Mellor. Published by the American Institute of Aeronautics and Astronautics, Inc., with permission.

\*Graduate Research Assistant, Department of Mechanical Engineering; currently Analyst, Enron International, P.O. Box 1188, Houston, TX 77251-1188.

†Centennial Professor of Mechanical Engineering. Associate Fellow AIAA.

eous fuel/air premixer model include air and fuel flow parameters and properties, and premixer geometry.

Hautman et al.<sup>7</sup> compared CFD predictions to experimental measurements of jet penetration and local mass fraction for a single transverse nitrogen jet injected into subsonic air flow in a rectangular test section. Quartz windows on the side and top of the test section allowed optical access. The mass distribution of the injected gas was determined via Mie scattering from titanium dioxide particles (diameter 1  $\mu\text{m}$ ) seeded into the gas injection stream. In general, Hautman et al. report that the CFD analysis predicted trends in jet penetration and spreading relatively well; however, the CFD significantly overpredicted the decay of maximum fuel mass fraction with downstream distance. Therefore, for the simple case of a single gaseous jet penetrating into a transverse airflow, these results indicate that CFD can only qualitatively predict fuel/air mixing. One must assume that quantitative CFD results would not improve in the case of modeling multiple fuel jets penetrating at various oblique angles into swirling airflow. Furthermore, in the case of modeling liquid fuel prevaporizing premixers, where initial conditions such as the droplet number, size distribution, and time mean and rms velocity vectors associated with each droplet must be estimated, only qualitative representations of liquid fuel premixing can be expected from CFD analysis.<sup>8</sup>

Currently, for the purposes of evaluating mixedness in gaseous premixers and liquid fuel prevaporizing premixers, only experimental diagnostic techniques can provide quantitative estimations of fuel/air mixing. It may also be possible to use such data to calibrate empirical expressions that could be used in the design process to calculate mixedness for a given configuration. Nevertheless, the fundamental investigation of fuel/air unmixedness effects begins with experimental measurements under practical test conditions. Techniques for measuring unmixedness experimentally are reviewed next.

#### Tracer Gas Measurements

Razdan et al.<sup>1</sup> measured the performance of two premixer configurations. The premixers were tested in an atmospheric-pressure, cold-flow rig. In these tests, a tracer gas consisting of a known mixture of natural gas and air was injected through the fuel holes, and localized samples of fuel/air mixture were collected with a traversing probe. The measured local mole fraction,  $C$ , of tracer gas was normalized by the mole fraction computed assuming perfect premixing of the total metered fuel/airflow through the premixer cup,  $C_{av}$ . Measurements were made at various radii and azimuthal positions in the premixer exit plane. The standard deviation in the fuel/air measurements for configuration 1 was about 12% of  $C_{av}$ , whereas for configuration 2 it was about 5.5% of  $C_{av}$ . Perfect premixing would correspond to a standard deviation of zero.

The types of measurements described in the preceding text can be used to compute local mixedness at different axial, radial, and circumferential positions in or at the exit of the premixer cup; however, probe measurements perturb the premixer flow, are susceptible to vibrations that can lead to spatial averaging of the measurements, and generally cannot resolve temporal fluctuations in mixedness. Optical techniques have been developed to circumvent the previously mentioned shortcomings of probe measurements.

#### Optical Techniques

Gulati and Warren<sup>9</sup> extended the work of Agarwal et al.<sup>10</sup> to measure fuel/air mixing via  $\text{NO}_2$  laser-induced fluorescence (LIF) in moderate-pressure (less than 15 atm), cold-flow systems. In this technique natural gas fuel is simulated by nitrogen seeded with  $\text{NO}_2$ . Nitrogen is used instead of methane to enhance LIF signal strength and linearity. Fric<sup>4</sup> used the  $\text{NO}_2$  LIF technique to measure atmospheric, cold-flow fuel/air mixing. LIF measurements were sampled at a rate of approximately 20 kHz, thus, spatial and temporal variations in local fuel/air concentration were measured.

Gulati and Warren<sup>9</sup> note that some disadvantages associated with the  $\text{NO}_2$  LIF method are as follows:

1) Because of the dissociation of  $\text{NO}_2$  at high temperatures, the LIF technique can only be used in cold flow at temperatures less than 500 K.

2) The  $\text{NO}_2$  LIF cannot be used at a pressure greater than 15 atm.

3)  $\text{NO}_2$  is toxic, and extreme precautions are required during testing.

Another optical method for measuring mixedness is the cold-flow, Mie-scattering technique of Hautman et al.<sup>7</sup> described earlier. This technique can be considered as essentially nonintrusive because the length scale of the seed particles is less than the Kolmogorov scale of turbulence in the experimental flow. Mongia et al.<sup>11</sup> discuss the development and validation (at pressures up to 10 atm in cold  $\text{CH}_4$ /airflow) of an inexpensive optical probe technique that measures fuel concentration directly via He-Ne laser absorption. Spatial resolution considerations require the use of fiber optics, so this method is intrusive. To summarize, the current techniques discussed earlier for measuring mixedness are generally not capable of use during combustor testing, and it is not immediately clear how to relate these cold-flow measurements of mixedness to the global performance of a combustor at fired, high-pressure (typically >15 atm), high-inlet temperature ( $\sim 700$  K) operating conditions.

For the purposes of premixer testing and modification, it is desirable to develop a simple, consistent method of quantifying fuel/air mixedness under realistic combustor operating conditions. Therefore, an alternative method of determining mixedness with the combustor fired is discussed next.

#### Estimation of Unmixedness from $\text{NO}_x$ Measurements

If it is assumed that LP  $\text{NO}_x$  emissions index (g  $\text{NO}_2/\text{kg}$  fuel) can be expressed in terms of a global fluid mechanic time ( $\tau_{sl,mo}$ ) and chemical kinetic time ( $\tau_{rno}$ ) as follows<sup>12</sup>:

$$\text{NO}_x \text{EI} = m |_{\phi < 1} (\tau_{sl,rno} / \tau_{rno}) \quad (1)$$

where  $m$  is a constant determined by linear regression analysis of a given set of experimental data, then for a given datum set in which the global fluid mechanic time for LP  $\text{NO}_x$  is the only independent variable at a given LP flame temperature ( $T_{\phi,m}$ )

$$\text{NO}_x \text{EI} / \tau_{sl,rno} |_{T_{\phi,m}} \propto 1 / \tau_{rno} |_{T_{\phi,m}} = \text{const} |_{T_{\phi,m}} \quad (2)$$

The preceding constraint should be satisfied for the data shown in Fig. 1 in which the fluid mechanic time is the only variable (because of the difference in airflow rate between the two datum series) at a given flame temperature. The data were collected from a gas-fired, can-type, LP gas-turbine combustor, combustor A, at a constant inlet temperature and pressure. See Barnes et al.<sup>13</sup> and Barnes and Mellor<sup>12</sup> for a more detailed discussion of the experimental combustor data and the experimental setup used in their collection. For the full set of data,  $8 \leq p_{in} \leq 14$  atm,  $550 \leq T_{in} \leq 750$  K,  $\tau_{res} = 13$  or 23 ms, and  $0.5 \leq \phi \leq 0.8$ . However, the combustor A data in Fig. 1 do not satisfy Eq. (2).

One possible interpretation of this is that the level of unmixedness, which is not accounted for in Eq. (2), is a variable between the two datum sets shown in Fig. 1, i.e., the LP  $\tau_{res}$  1 data have the shorter residence time and thus the higher rms velocity in the premixer and higher mixedness. As discussed in Barnes and Mellor,<sup>12</sup> if the main fuel and air mixture is not homogeneous, then a distribution of equivalence ratios exists in the LP flame. Following Mikus and Heywood<sup>14</sup> and Fletcher and Heywood,<sup>15</sup> it is assumed that this equivalence ratio distribution is Gaussian and is centered about the equivalence ratio computed assuming perfect premixing of the main fuel

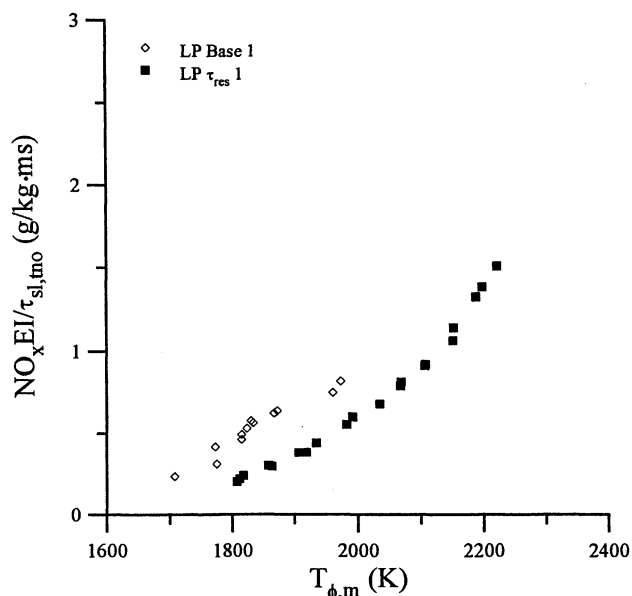


Fig. 1 Graph of combustor A LP  $NO_x$  data divided by corresponding  $NO_x$  fluid mechanic times ( $\tau_{sl,tmo}$ ). The open diamonds represent data obtained at a longer residence time than the closed squares. Inlet temperature and pressure are constant. The fact that the curves do not collapse indicates that unmixedness ( $s$ ) is a variable between the two datum sets.

and air. Therefore, the form of the probability density function (PDF) for eddies in the LP flame is

$$\Psi(\phi_{eddy}) = \frac{1}{s\bar{\phi}_m\sqrt{2\pi}} \exp \left[ -\frac{(\phi_{eddy}/\bar{\phi}_m - 1)^2}{2s^2} \right] \quad (3)$$

Here  $\bar{\phi}_m$  is the mean and  $\phi_{eddy}$  is the local equivalence ratio associated with an individual reacting eddy. The time-averaged standard deviation in equivalence ratio in the LP flame is  $\sigma_\phi$ , so that

$$s \equiv \sigma_\phi / \bar{\phi}_m \quad (4)$$

following Mikus and Heywood. A standard deviation of zero corresponds to the perfectly premixed case in which all eddies in the LP flame burn with the mean equivalence ratio. Individual eddy equivalence ratios ( $\phi_{eddy}$ ), which are greater than the mean, lead to increased  $NO_x$  emissions via the exponential decrease in the NO formation time with increasing eddy flame temperature.

Applying Eq. (3) to Eq. (1) one has

$$NO_x EI|_s = m|_{\phi < 1} \int_0^{1.4} \frac{\Psi(\phi_{eddy}) \tau_{sl,tmo}}{\tau_{no}(\phi_{eddy})} d\phi_{eddy} \quad (5)$$

The integrand represents NO formation in an individual eddy in the LP flame with an equivalence ratio of  $\phi_{eddy}$ . Equation (5) reduces to Eq. (1) when  $s$  approaches zero. The lower integration limit matches the lower limit of equivalence ratio, and for nominal combustor operating conditions, the upper integration limit of 1.4 is sufficient to capture greater than 99% of the integral over the range  $\pm \infty$ .<sup>12</sup>

To estimate the level of unmixedness in the LP base 1 data, it is assumed that the LP  $\tau_{res}$  1 data correspond to perfectly premixed operating conditions ( $s = 0$ ). Equation (1) is calibrated such that it fits the LP  $\tau_{res}$  1 data (Fig. 2). Next, the perfectly premixed model for the LP  $\tau_{res}$  1 data is modified following Eq. (5) by increasing  $s$  such that the base 1 data are correlated. As shown in Fig. 2, this process reveals that  $s$  is on the order of 0.35 for the LP base 1 data. Note that for a

premixed flame temperature greater than  $\sim 2000$  K, the model predicts the sensitivity of  $NO_x$  to decrease with increasing temperature. This occurs as the fraction of the eddies with  $\phi_{eddy}$  greater than one increases with an increasing mean equivalence ratio, thus leading to lower local flame temperatures. Magruder et al.<sup>16</sup> note that the same trend is apparent in the high-temperature ( $>2000$  K) LP  $NO_x$  data of Roffe and Venkataramani.<sup>17</sup>

The technique of estimating unmixedness discussed earlier is similar to another technique that is often used where LP  $NO_x$  measurements are compared to the "perfectly premixed" data of Leonard and Stegmaier.<sup>5</sup> This technique is illustrated in Fig. 3. Here, the best fit of the Leonard and Stegmaier data is taken as the perfectly premixed ( $s = 0$ ) baseline. As in the method in Fig. 2, a distribution in equivalence ratio is assumed such that the baseline model with  $s$  greater than zero correlates the experimental data of concern. Increasing values of  $s$  used to correlate the experimental data correspond to increasing unmixedness and larger displacements between the Leonard and Stegmaier data and the experimental data in question.

Using the preceding techniques, estimates of unmixedness can be deduced from experimental  $NO_x$  data. However, some

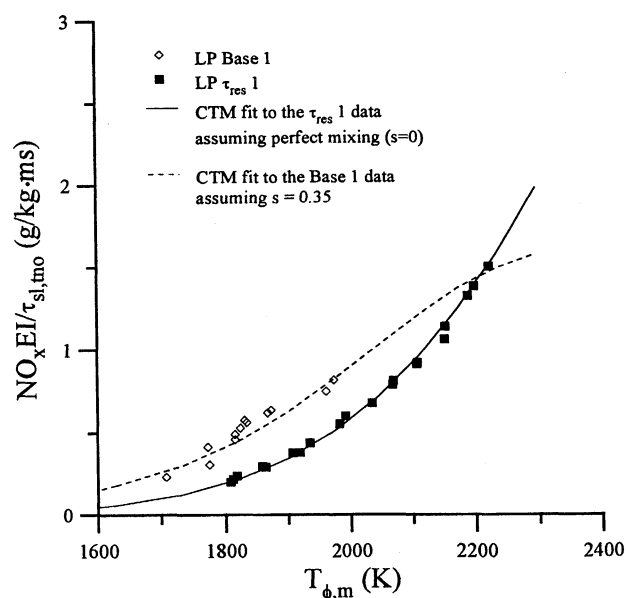


Fig. 2 Using the best-fit through the LP  $\tau_{res}$  1 data for the perfectly premixed baseline in Eq. (1),  $s$  is adjusted such that the LP  $\tau_{res}$  1 best-fit correlates the LP base 1 data. The value of  $s$  corresponding to the LP base 1 data is estimated to be 0.35.

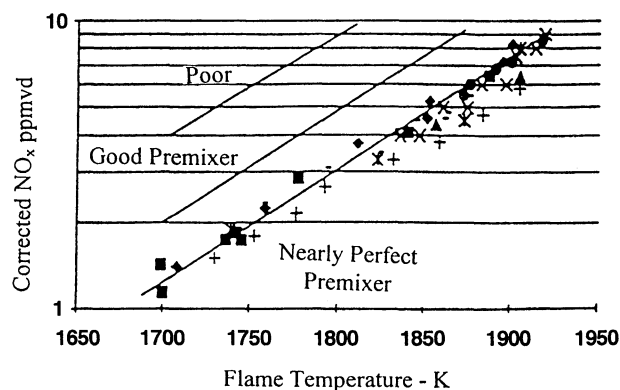


Fig. 3 Schematic showing the best-fit through the Leonard and Stegmaier data.<sup>5</sup> The Leonard and Stegmaier best-fit is used as the perfectly premixed ( $s = 0$ ) baseline in this case. The two other example trendlines correspond to experimental data with  $s$  greater than zero.<sup>5</sup>

ambiguities exist with these two methods. First, either temporal or spatial unmixedness leads to elevated  $\text{NO}_x$  emissions, and exhaust plane gas sampling cannot elucidate which is responsible.† Schlegel et al.<sup>18</sup> argue, however, that temporal fluctuations simply represent spatial unmixedness along a mean axial streamline.

Second, in the case of the analysis in Fig. 2, it is unlikely that the LP  $\tau_{\text{res}}$  1 baseline data are perfectly premixed. Therefore, 0.35 is at best an estimate of the relative difference in  $s$ , and the absolute values of  $s$  cannot be computed. In the case of the analysis shown in Fig. 3, Leonard and Stegmaier report that their  $\text{NO}_x$  data are independent of combustor inlet pressure and temperature, probe position, and premixer geometry. In theory, these trends may be true for gas-fired, perfectly premixed combustors, but they are certainly not true for gas-fired, practical LP combustors.<sup>13</sup> Therefore, in the analysis shown in Fig. 3, the distance between the baseline and any of the experimental data trendlines is a function not only of unmixedness, but also combustor inlet temperature and pressure, residence time, and combustor geometry. In fact, De Pietro et al.<sup>19</sup> use a quantitative chart like Fig. 3, for one combustor inlet pressure and temperature, that suggests Leonard and Stegmaier's data actually correspond to  $s$  values of approximately 0.08 at their lower flame temperatures and about 0.07 at the higher values. Accordingly, it is difficult to make an accurate estimate of unmixedness using the technique shown in Fig. 3.

In the next section, a method of deducing unmixedness from experimental CO measurements is proposed. Like the methods described in Figs. 2 and 3, this technique can be applied to estimate unmixedness in practical LP combustors under fired conditions. Furthermore, the relationship between the experimental data and the perfectly premixed baseline is significantly more simple than that in Figs. 2 and 3.

### CO Emissions from Lean Premixed Combustors

Before discussing the technique for computing unmixedness with combustor CO emissions measurements, the characteristic trends of experimental CO measurements with changing combustor equivalence ratio (chemical kinetics) and residence time (fluid mechanics) are reviewed. Sheppard<sup>20</sup> considered  $\text{CO} + \text{OH} \leftrightarrow \text{CO}_2 + \text{H}$  and computed these dependencies as functions of both unmixedness and combustor operating conditions. For perfect mixing, qualitative trends for CO vs main equivalence ratio at two different residence times are shown in Fig. 4. Lower equivalence ratios yield lower flame temperatures in the combustor that do not promote substantial CO oxidation through the  $\text{CO} + \text{OH}$  reaction before quenching occurs. As the mean equivalence ratio is increased, the kinetic time for CO oxidation decreases, and CO levels approach equilibrium values before quenching occurs. Further increases in equivalence ratio past the intersection of the kinetic and equilibrium regimes ( $\phi^*$ ) leads to higher flame temperatures that promote  $\text{CO}_2$  dissociation through the  $\text{CO}_2 + \text{H}$  reaction and thus higher CO levels. Therefore, CO levels are dominated by oxidation kinetics when the equivalence ratio is less than  $\phi^*$  and by equilibrium when greater than or equal to  $\phi^*$ . Figure 4 also indicates that while the equilibrium CO trend is fixed for a given fuel type, inlet pressure, and inlet temperature of the fuel and air, the kinetic CO curve shifts down as the combustor residence time is increased. Therefore,  $\phi^*$  shifts to the left as the combustor residence time is lengthened.

Measured CO emissions that correspond to the kinetic and CO equilibrium regimes in Fig. 4 have been presented in recent literature. For example, data from the single, quartz-lined burner of Lovett and Mick<sup>21</sup> are shown in Fig. 5 in the form of an emissions tradeoff plot. On this type of graph,  $\text{NO}_x$  is proportional to mean equivalence ratio. Inlet conditions are constant along each of the curves shown in Fig. 5. The CO

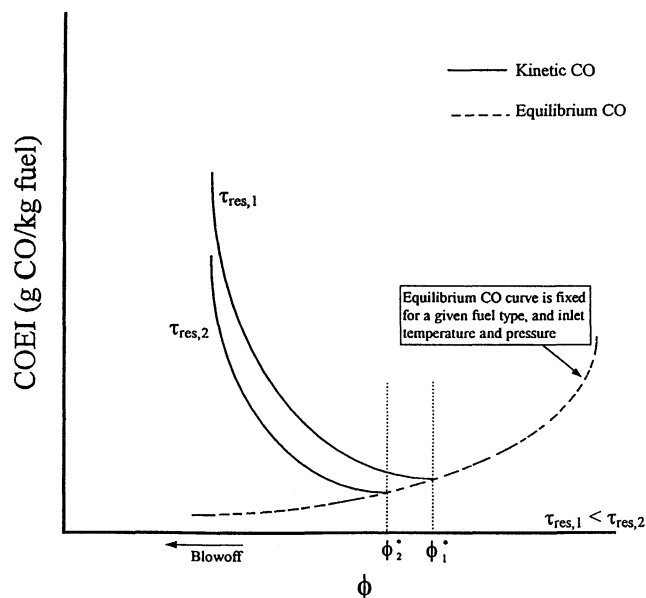


Fig. 4 Qualitative trends in perfectly premixed lean combustor CO emissions vs. premixer equivalence ratio for two different residence times ( $\tau_{\text{res},1}$  and  $\tau_{\text{res},2}$ ). Fuel type, inlet pressure, and inlet fuel and air temperature are constant. The dashed lines through the intersections of the kinetic and equilibrium CO curves separate the two regimes of CO chemistry. For each respective residence time,  $\phi^*$  delineates the regime where the reaction  $\text{CO} + \text{OH}$  limits the oxidation of CO, on the left, from the equilibrium regime on the right.

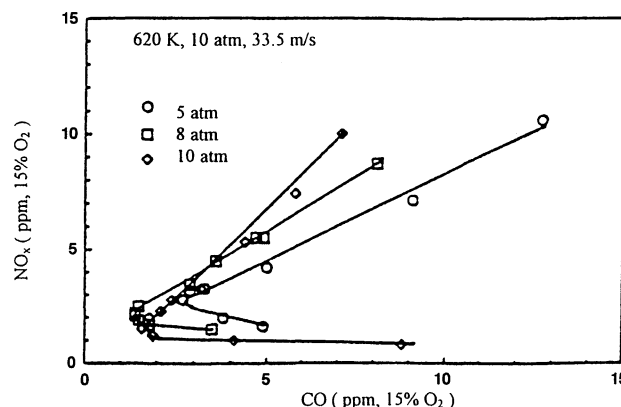


Fig. 5 Experimental CO and  $\text{NO}_x$  data of Lovett and Mick<sup>21</sup> shown on an emissions tradeoff plot. On this type of graph  $\text{NO}_x \sim \phi$ . Regions of kinetic and equilibrium CO (see Fig. 4) are apparent. The operating conditions shown in the upper left-hand corner of the graph should read "620 K, 33.5 m/s"; "10 atm" is a typographical error.

data at the  $\text{NO}_x$  levels below and above the minimum for each curve correspond to the kinetic and equilibrium regimes in Fig. 4, respectively. Note that in the latter regime, there is no classical  $\text{NO}_x/\text{CO}$  tradeoff: both emissions increase with increasing premixer mean equivalence ratio. The data that will be focused on here are from the experiments of Joshi et al.<sup>2</sup>

Joshi et al. used several different test-rig configurations to evaluate the double annular counter rotating swirler (DACRS) premixer. Tests were performed with natural gas under conditions representative of those in aeroderivative turbines. CO emissions measurements taken from the single cup test rig shown in Fig. 6a are the focus of the work here. The rig was configured with the DACRS II premixer shown in Fig. 6b and an uncooled, high-temperature ceramic wall with no air addition sites downstream of the dome exit. Reference velocity was held constant at approximately 12 m/s during testing. Emis-

†Fric, T. F., General Electric Corporate Research and Development, Personal Communication, June 1997.

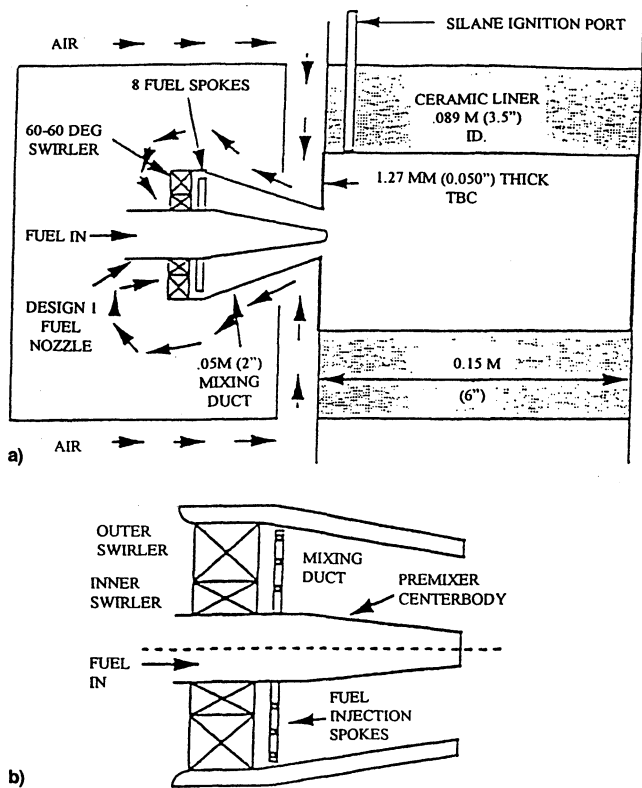


Fig. 6 a) Single cup test combustor cross section and b) DACRS II premixer cross section.<sup>2</sup>

sions were measured along the combustor centerline with an aero-quench probe designed according to the guidelines of Roffe and Venkataramani.<sup>22</sup>

Exhaust-plane CO measurements from the 620 K, 5-atm tests were digitized from Joshi et al. and are shown in Fig. 7, where one low datum believed erroneous is excluded from further analysis here. The remaining data clearly correspond to the equilibrium CO regime in Fig. 4. Furthermore, probe measurements along the combustor axis made by Joshi et al. indicated that CO levels reached an equilibrium state, i.e., the axial gradient of CO concentration approached zero, about 0.1 m downstream of the premixer exit (see Fig. 6a).

The experimental data in Fig. 7 are also compared with the equilibrium COEI computed with STANJAN<sup>23</sup> at the fully mixed main equivalence ratio for an assumed natural gas composition ( $H/C = 3.8$ ). In a combustor where CO reaches equilibrium upstream of the probe location, the measured COEI should correspond to the computed equilibrium COEI. In Fig. 7 the computed COEI curve for pure propane ( $H/C = 2.7$ ) is used as an upper limit to show that the discrepancy between measured and equilibrium CO cannot be attributed to the assumed fuel type. Similarly, a natural gas preheat temperature of 500 K is used as an upper limit to show that the discrepancy is not because of an assumed fuel inlet temperature.

Finally, +2% error bars are shown to indicate that the difference is not because of an error in the actual vs nominal fuel/air ratio. Using Fig. 7 as an example, one can see that translating a given datum point left or right, parallel to the  $x$  axis, to simulate an uncertainty in the fuel/air ratio measurement, corresponds to an exponential widening or narrowing of the vertical distance to the equilibrium CO curve. Assuming nominal combustor operating pressures and temperatures at an equivalence ratio of approximately 0.6, uncertainties between  $\pm 1$  and 2% in fuel/air ratio correspond to uncertainties in  $s$  between  $\pm 4$  and 12%, respectively. Therefore, control of laboratory fuel/air ratio measurement accuracy is of paramount importance in applying this technique of unmixedness determination.

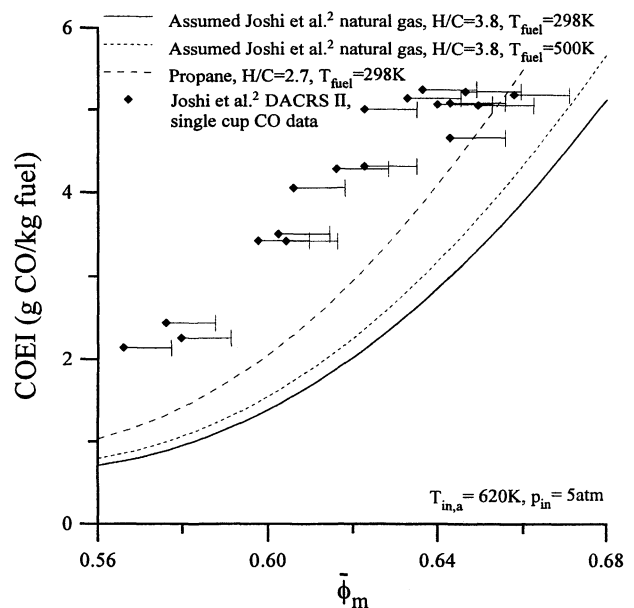


Fig. 7 Digitized CO data of Joshi et al.<sup>2</sup> for  $T_{in} = 620$  K,  $p_{in} = 5$  atm, and constant reference velocity. The propane equilibrium curve is used as an upper limit to show that the discrepancy between measured and equilibrium CO cannot be attributed to the assumed natural gas composition. A natural gas preheat temperature of 500 K is used as an upper limit to show that the discrepancy is not because of assumed fuel inlet temperature. +2% error bars are shown to indicate that the difference is not because of an error in the fuel/air measurement.

Because only the nominal operating conditions and natural gas composition are available for the Joshi et al. data,<sup>2</sup> one must assume that the discrepancy between the measured and equilibrium COEI in Fig. 7 is an indication of unmixedness. It is also thought that the solid computed equilibrium CO curve corresponds most closely to the actual test conditions of Joshi et al. and, therefore, this case is taken as the perfectly premixed baseline ( $s = 0$ ). Nevertheless, the technique of estimating unmixedness from the displacement between measured and equilibrium CO curves for combustors in general will be illustrated with the Joshi et al. data.

### Evaluating Mixedness with CO Emission Measurements

As in the  $NO_x$  model discussed earlier, unmixedness is modeled as a distribution of equivalence ratios associated with the reacting eddies convecting through the combustor. However, in this case, one is concerned with CO emissions that exceed equilibrium values because of unmixedness. Equation (3) is graphed in Fig. 8 along with the baseline equilibrium COEI curve from Fig. 7. As shown in Fig. 8, it is the increase in temperature associated with the richer eddies that leads to the increase in equilibrium CO and, thus, increased CO emissions, if the mean equivalence ratio is greater than  $\phi^*$ . Equation (3) is used to weight the equilibrium values over the reacting eddies passing through the emissions measurement plane in the combustor to compute the total COEI for any mean equivalence ratio and  $s$

$$COEI(\bar{\phi}_m)|_{eq,s} = \int_0^{1.4} \Psi(\phi_{eddy}) COEI|_{eq} d\phi_{eddy} \quad (6)$$

( $COEI|_{eq}$ ) is represented with a piecewise polynomial fit, and the integration limits are selected following the reasoning discussed with respect to Eq. (5).

To quantify unmixedness for the data shown in Fig. 7, the  $s$  parameter in Eq. (6) is adjusted such that Eq. (6) is equal to

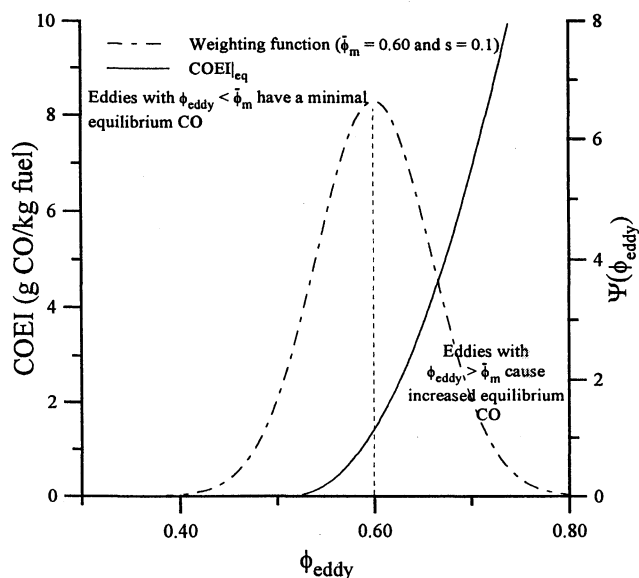


Fig. 8 Graph indicating the relationship between a typical Gaussian eddy equivalence ratio distribution and the equilibrium CO curve for the inlet conditions of the data in Fig. 7.

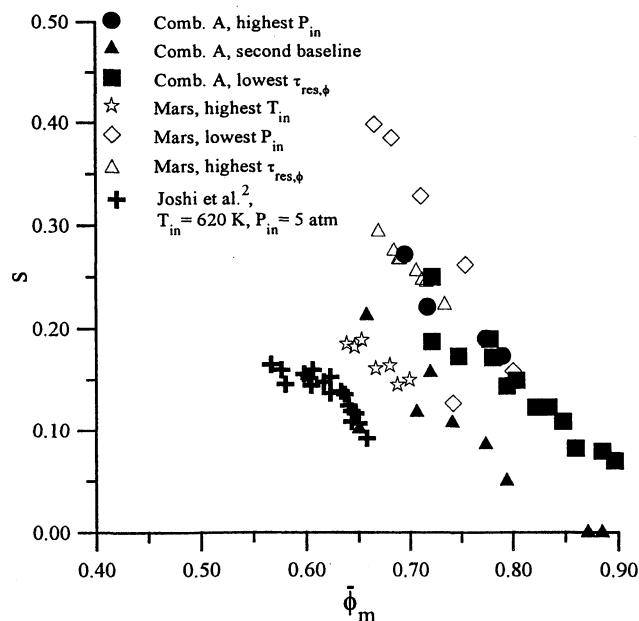


Fig. 9 Unmixedness levels deduced from CO emissions [Eq. (6)] for the 620 K, 5-atm tests of Joshi et al.<sup>2</sup> shown in Fig. 7, the Mars premixer, and for selected combustor A operating conditions.<sup>24</sup>

the measured CO at each value of mean equivalence ratio. The computed values of  $s$  for the Joshi et al. data<sup>2</sup> in Fig. 7 are shown in Fig. 9. Also presented in Fig. 9, taken from Mello et al.,<sup>24</sup> are data for selected combustor A run conditions<sup>12,13</sup> and for the Mars premixer, which was tested in the facilities of Solar Turbines (see Ref. 24). Unlike the rig of Joshi et al., both the single-injector combustor on which the Mars premixer was tested and combustor A are film-cooled. Consequently, Mello et al. assume equilibrium obtains at the overall equivalence ratio, i.e., at the burner outlet temperature, for the CO measured vs equilibrium analysis of unmixedness in both the Mars configuration and combustor A.

In contrast to the deduction of the  $s$  parameter independent of  $\phi$  based on the  $\text{NO}_x$  methodology of Fig. 2, the values of unmixedness parameter for all three combustors presented in Fig. 9 vary inversely with premixer mean equivalence ratio. This observation suggests that mixing is enhanced as the linear

momentum of the fuel jets to the airflow in the premixer, i.e., the penetration of the fuel jets, is increased. Additionally, the results in Fig. 9 imply a strong influence of premixer design with a weaker effect of air inlet conditions on unmixedness. Mello et al. analyze the Mars and combustor A data in more depth, as well as the quantitative uncertainties in unmixedness that result if the temperature at which CO attains equilibrium is unknown.

## Conclusions

The principal advantages of deducing unmixedness for a given set of LP combustor data from CO measurements over current techniques are as follows:

1) Low cost: Unmixedness can be measured during fired combustor rig tests via standard emissions measurement instrumentation.

2) Nonintrusive: The fluid mechanics and chemical kinetics associated with CO oxidation and CO equilibrium in the LP combustor are not affected by exhaust plane probe measurements.

3) Adaptive: The method can be applied to a rig configured with a single or multiple premixer nozzles.

However, because it is based on probe or rake measurements, it cannot distinguish spatial and temporal unmixedness. In addition, application of the technique is subject to some constraints:

1)  $\bar{\phi}_m \geq \phi^*$ : Recalling the trends shown in Fig. 4, the technique can only be applied to estimate unmixedness for operating conditions in the CO equilibrium regime above  $\phi^*$ . This condition typically does not apply to nominal, full-power LP combustor operating conditions. Therefore, in practice it is likely that estimates of unmixedness for operating conditions below  $\phi^*$  will have to be extrapolated from unmixedness measurements above  $\phi^*$ , and from idle to full load conditions. This issue can be addressed only via future experimental work.

2) Little or no airflow other than that through the premixer: In addition to the data of Joshi et al.<sup>2</sup> and Lovett and Mick,<sup>21</sup> other examples of LP CO equilibrium data taken from flameholder and combustor rigs above  $\phi^*$  include Snyder et al.<sup>3</sup> and Puri et al.<sup>25</sup> However, to perform the unmixedness analysis with the CO measurements, the temperature associated with equilibrium must be easily defined. In the case of the Joshi et al.<sup>2</sup> tests (see also Snyder et al.<sup>3</sup>), the rig was configured with a ceramic liner with no air addition downstream of the premixer exit plane, i.e., 100% of the combustor airflow passed through the LP flame. Thus, the premixer flame temperature at the mean equivalence ratio is used to characterize the thermal environment in which equilibrium is obtained in the combustor. If air is added through film-cooling slots or dilution holes (such as in the Mars premixer rig and combustor A, data for which are shown in Fig. 9, and the rigs of Lovett and Mick<sup>21</sup> and Puri et al.<sup>25</sup>), the temperature associated with CO equilibrium may be closer to that at the burner outlet. In this case, even for  $s$  greater than zero, equilibrium CO levels may be below [ $\ll 1$  parts per million by volume, dry (ppmvd)] the accuracy of CO instrumentation.<sup>13,24</sup> Therefore, the ideal combustor configuration for use with the CO unmixedness method is a premixer attached to a ceramic, nearly adiabatic combustor liner with no film-cooling slots or dilution holes, e.g., those of Joshi et al.<sup>2</sup> and Snyder et al.<sup>3</sup> For a LP combustor, such a liner is a necessity because it allows for more efficient use of combustor airflow to reduce the premixed flame temperature and LP  $\text{NO}_x$ . These observations indicate that constraint (2) is consistent with state-of-the-art LP technology.

3) Adequate quenching of CO reactions in the sampling rake or probe: Failure to freeze the CO chemistry at combustor conditions will lead to incorrect conclusions regarding premixer performance.

If LP CO data are measured in a practical combustor rig that satisfies the operating constraints listed earlier, the premixer designer should observe the qualitative equilibrium trends in-

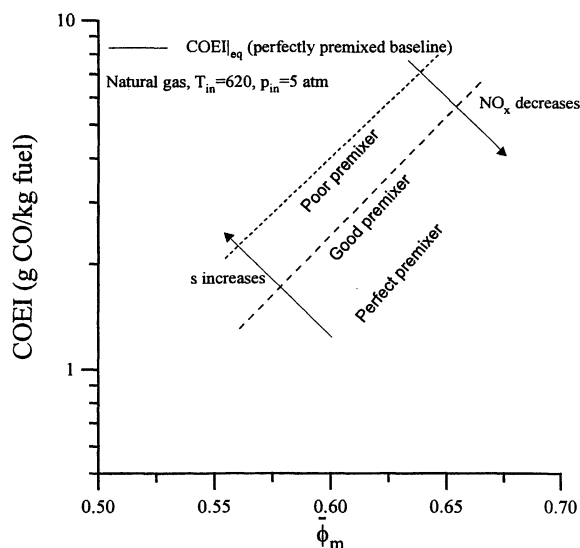


Fig. 10 Expected trends in measured COEI with  $s$  for mean equivalence ratio greater than  $\phi^*$ . The baseline case corresponds to equilibrium at  $s = 0$ .

indicated in Fig. 10. This graph is analogous to that shown in Fig. 3; however, it is believed that unmixedness is the only variable between the baseline equilibrium curve and the measured curves at a given premixed mean flame temperature. Therefore, accurate estimates of  $s$  should be possible following Eq. (6).

### Acknowledgments

This paper was prepared with the support of the U.S. Department of Energy, Morgantown Energy Technology Center, under cooperative agreement DE-FC21-92MC29061. L. P. Golan and D. Fant of the Advanced Gas Turbine Systems Research Program at the South Carolina Energy R&D Center served as technical monitors. An early version of the paper was presented as ASME 97-GT-73.

### References

- <sup>1</sup>Razdan, M. K., McLeroy, J. T., and Weaver, W. E., "Retrofittable Dry Low Emissions Combustor for 501-K Industrial Gas Turbine Engines," American Society of Mechanical Engineers, Paper 94-GT-439, June 1994.
- <sup>2</sup>Joshi, N. D., Epstein, M. J., Durlack, S., Marakovits, S., and Sabla, P. E., "Development of a Fuel/Air Premixer for Aero-Derivative Dry Low Emissions Combustors," American Society of Mechanical Engineers, Paper 94-GT-253, June 1994.
- <sup>3</sup>Snyder, T. S., Rosfjord, T. J., McVey, J. B., Hu, A. S., and Schlein, B. C., "Emissions and Performance of a Lean-Premixed Gas Fuel Injection System for Aeroderivative Gas Turbine Engines," American Society of Mechanical Engineers, Paper 94-GT-234, June 1994.
- <sup>4</sup>Fric, T. F., "Effects of Fuel-Air Unmixedness on  $\text{NO}_x$  Emissions," *Journal of Propulsion and Power*, Vol. 9, No. 5, 1993, pp. 708–713.
- <sup>5</sup>Leonard, G., and Stegmaier, J., "Development of an Aeroderivative Gas Turbine Dry Low Emissions Combustion System," *Transactions of the American Society of Mechanical Engineers*, Vol. 116, No. 3, 1994, pp. 542–546.

- <sup>6</sup>Jones, W. P., and Launder, B. E., "The Prediction of Laminarization with a 2-Equation Model of Turbulence," *International Journal of Heat and Mass Transfer*, Vol. 15, No. 2, 1972, pp. 301–312.
- <sup>7</sup>Hautman, D. J., Haas, R. J., and Chiappetta, L., "Transverse Gaseous Injection into Subsonic Air Flows," AIAA Paper 91-0576, Jan. 1991.
- <sup>8</sup>Snyder, T. S., Rosfjord, T. J., McVey, J. B., and Chiappetta, L. M., "Comparison of Liquid Fuel/Air Mixing and  $\text{NO}_x$  Emissions for a Tangential Entry Nozzle," American Society of Mechanical Engineers, Paper 94-GT-283, June 1994.
- <sup>9</sup>Gulati, A., and Warren, R. E., " $\text{NO}_2$ -Based Laser-Induced Fluorescence Technique to Measure Cold-Flow Mixing," *Journal of Propulsion and Power*, Vol. 10, No. 1, 1994, pp. 54–61.
- <sup>10</sup>Agarwal, Y., Hadeishi, T., and Robben, F., "Measurement of  $\text{NO}_2$  Concentration in Combustion Using Fluorescence Excited by an Argon-Ion Laser," AIAA Paper 76-136, Jan. 1976.
- <sup>11</sup>Mongia, R., Tomita, E., Hsu, F., Talbot, L., and Dibble, R., "Optical Probe for In-Situ Measurements of Air-to-Fuel Ratio in Low Emission Engines," AIAA Paper 96-0174, Jan. 1996.
- <sup>12</sup>Barnes, J. C., and Mellor, A. M., "Effects of Unmixedness in Piloted-Lean Premixed Gas-Turbine Combustors," *Journal of Propulsion and Power*, Vol. 14, No. 6, 1998, pp. 967–973.
- <sup>13</sup>Barnes, J. C., Mello, J. P., Mellor, A. M., and Malte, P. C., "Preliminary Study of  $\text{NO}_x$ , CO, and Lean Blowoff in a Piloted-lean Premixed Combustor. Part I: Experimental; Part II: Modeling," Technical Meeting, Central States Section, The Combustion Inst., St. Louis, MO, May 1996 (Papers 31 and 32).
- <sup>14</sup>Mikus, T., and Heywood, J. B., "The Automotive Gas Turbine and Nitric Oxide Emissions," *Combustion Science and Technology*, Vol. 4, Dec. 1971, pp. 149–158.
- <sup>15</sup>Fletcher, R. S., and Heywood, J. B., "A Model for Nitric Oxide Emissions from Aircraft Gas Turbine Engines," AIAA Paper 71-123, Jan. 1971.
- <sup>16</sup>Magruder, T. D., McDonald, J. P., Mellor, A. M., Tonouchi, J. H., Nicol, D. G., and Malte, P. C., "Engineering Analysis for Lean Premixed Combustor Design," AIAA Paper 95-3136, July 1995.
- <sup>17</sup>Roffe, G., and Venkataramani, K. S., "Experimental Study of the Effects of Flameholder Geometry on Emissions and Performance of Lean Premixed Combustors," NASA CR-135424, June 1978.
- <sup>18</sup>Schlegel, A., Streichsbier, M., Mongia, R., and Dibble, R., "A Comparison of the Influence of Fuel/Air Unmixedness on  $\text{NO}_x$  Emissions in Lean Premixed, Non-Catalytic and Catalytically Stabilized Combustion," American Society of Mechanical Engineers, Paper 97-GT-306, June 1997.
- <sup>19</sup>De Pietro, S. M., Noden, R. M., Hesse, H., Hornsby, C., and Norster, E. R., "Development of a Dry Low  $\text{NO}_x$  Combustion System for the EGT Typhoon," *Power-Gen '96, Book III, Generation Trends*, Vol. 9, Gas Turbine Technologies, PennWell, Houston, TX, Dec. 1996, pp. 481–500.
- <sup>20</sup>Sheppard, C. G. W., "A Simple Model for Carbon Monoxide Oxidation in Gas Turbine Combustors," *Combustion Science and Technology*, Vol. 11, July 1975, pp. 49–56.
- <sup>21</sup>Lovett, J. A., and Mick, W. J., "Development of a Swirl and Bluff-Body Stabilized Burner for Low- $\text{NO}_x$  Lean-Premixed Combustion," American Society of Mechanical Engineers, Paper 95-GT-166, June 1995.
- <sup>22</sup>Roffe, G., and Venkataramani, K. S., "Emissions Measurements for a Lean Premixed Propane/Air System at Pressures up to 30 Atmospheres," NASA CR-159421, June 1978.
- <sup>23</sup>Reynolds, W. C., "STANJAN Version 3.93," Dept. of Mechanical Engineering, Stanford Univ., Stanford, CA, 1987.
- <sup>24</sup>Mello, J. P., Mellor, A. M., Steele, R. C., and Smith, K. O., "A Study of the Factors Affecting  $\text{NO}_x$  Emissions in Lean Premixed Turbine Combustors," AIAA Paper 97-2708, July 1997.
- <sup>25</sup>Puri, R., Stansel, D. M., Smith, D. A., and Razdan, M. K., "Dry Ultra-Low  $\text{NO}_x$  'Green Thumb' Combustor for Allison's 501-K Series Industrial Engines," American Society of Mechanical Engineers, Paper 95-GT-406, June 1995.